J|A|C|S
ARTICLES
Published on Web 03/03/2002

Hoogsteen-Based Parallel-Stranded Duplexes of DNA. Effect of 8-Amino-purine Derivatives

Elena Cubero,[†] Anna Aviñó,[‡] Beatriz G. de la Torre,[§] Miriam Frieden,[‡] Ramón Eritja,*[,§] F. Javier Luque,[||] Carlos González,[⊥] and Modesto Orozco*[,†]

Contribution from Departament de Bioquímica i Biologia Molecular, Facultat de Química, Universitat de Barcelona, Martí i Franquès 1, Barcelona 08028, Spain, Cygene Spain S. L. Parc Científic de Barcelona, Baldiri i Reixac, 10-12, Barcelona 08028, Spain, Instituto de Biología Molecular de Barcelona, C. S. I. C., Jordi Girona 18-26, Barcelona 08034, Spain, Departament de Fisicoquímica, Facultat de Farmàcia, Universitat de Barcelona, Avgda Diagonal sn. Barcelona 08028, Spain, and Instituto de Estructura de la Materia, C. S. I. C., C/Serrano 119, Madrid 28006, Spain

Received August 9, 2001. Revised Manuscript Received October 18, 2001

Abstract: The structure of parallel-stranded duplexes of DNA-containing a mixture of guanines (G) and adenines (A) is studied by means of molecular dynamics (MD) simulation, as well as NMR and circular dichroism (CD) spectroscopy. Results demonstrate that the structure is based on the Hoogsteen motif rather than on the reverse Watson−Crick one. Molecular dynamics coupled to thermodynamic integration (MD/TI) calculations and melting experiments allowed us to determine the effect of 8-amino derivatives of A and G and of 8-amino-2′-deoxyinosine on the stability of parallel-stranded duplexes. The large stabilization of the parallel-stranded helix upon 8-amino substitution agrees with a Hoogsteen pairing, confirming MD, NMR, and CD data, and suggests new methods to obtain DNA triplexes for antigene and antisense purposes.

Introduction

DNA can form a large range of helical structures including duplexes, triplexes, and tetraplexes.[1−5] The right-handed B-type duplex is the most common structure of DNA, but even now, decades after the discovery of the B-DNA,[6] new double helical conformations of DNA are being described.[7,8] This demonstrates that DNA has great flexibility and exhibits a large polymorphism depending on sequence, chemical modifications, or alterations in the DNA environment.[1]

Most DNA duplexes, including the well-known B and A forms, are antiparallel (i.e., one strand runs 5′ → 3′ and the other 3′ → 5′), but parallel arrangements have been found in both hairpins and linear DNAs.[9−19] Sequences with propensity to form parallel DNAs haven been found in specific chromosome regions,[20−25] and could have an evolutionary role.[26] Moreover, certain types of parallel-stranded DNA can be excellent templates for the formation of triplexes. This can be very useful for biotechnological purposes, as well as for the development of antigene (targeting of genetic DNA by an artificial oligonucleotide) and antisense (targeting of natural messenger RNA by an artificial oligonucleotide) therapies.[27−29]

* Corresponding authors.
[†] Departament de Bioquímica i Biologia Molecular, Facultat de Química, Universitat de Barcelona.
[‡] Cygene Spain S. L. Parc Científic de Barcelona.
[§] Instituto de Biología Molecular de Barcelona, C.S.I.C.
[||] Departament de Fisicoquímica, Facultat de Farmàcia, Universitat de Barcelona.
[⊥] Instituto de Estructura de la Materia, C.S.I.C.

(1) Saenger, W. *Principles of Nucleic Acid Structure*; Springer: New York, 1994.
(2) Soyfer, V. N.; Potaman, V. N. *Triple Helical Nucleic Acids*; Springer: New York, 1996.
(3) Sun, J. S.; Hélène, C. *Curr. Opin. Struct. Biol.* 1993, *3*, 345.
(4) Laughlan, G.; Murchie, A. I.; Norman, M. H.; Moody, P. C.; Lilley, D. M.; Luisi, B. *Science* **1994**, *265*, 520.
(5) Williamson, J. R. *Annu. Rev. Biophys. Biomol. Struct.* **1994**, *23*, 703.
(6) Watson, J. D.; Crick, F. H. C. *Nature* **1953**, *171*, 737.
(7) Ng, H.-L.; Kopka, M. L.; Dickerson, R. E. *Proc. Natl. Acad. Sci. U.S.A.* **2000**, *97*, 2035.
(8) Vargason, J. M.; Eichman, B. F.; Ho, P. S. *Nature Struct. Biol.* **2000**, *7*, 758.
(9) Rippe, K.; Jovin, T. M. *Methods Enzymol.* **1992**, *211*, 199.
(10) Van de Sande, J. H.; Ramsing, N. B.; Germann, M. W.; Elhorst, W.; Kalisch, B. W.; Kitzing, E. V.; Pon, R. T.; Clegg, R. C.; Jovin, T. M. *Science* **1988**, *241*, 551.
(11) Ramsing, N. B.; Rippe, K.; Jovin, T. M. *Biochemistry* **1989**, *28*, 9528.
(12) Germann, M. W.; Vogel, H. J.; Pon. R. T.; van de Sande, J. H. *Biochemistry* **1989**, *28*, 6220.
(13) Rippe, K.; Ramsing, N. B.; Jovin, T. M. *Biochemistry* **1989**, *28*, 9536.
(14) Rentzeperis, D.; Rippe, K.; Jovin, T. M.; Marky, L. A. *J. Am. Chem. Soc.* **1992**, *114*, 5926.
(15) Germann, M. W.; Kalisch, B. W.; Pon, R. T.; van de Sande, J. H. *Biochemistry* **1990**, *29*, 9426.
(16) Lavelle, L.; Fresco, J. R. *Nucleic Acids Res.* **1995**, *23*, 2692.
(17) Scaria, P. V.; Shafer, R. H. *Biochemistry* **1996**, *35*, 10985.
(18) Bhaumik, S. R.; Kandala, V. R.; Govil, G.; Liu, K.; Miles, H. T. *Nucleic Acids Res.* **1995**, *23*, 4116.
(19) Liu, K.; Miles, T.; Frazier, J.; Sasisekharan, V. *Biochemistry* **1993**, *32*, 11802.
(20) Kan, C. H.; Zhang, R.; Ratliff, R.; Moyzis, R.; Rich, A. *Nature* **1992**, *356*, 126.
(21) Sen, D.; Gilbert, D. *Biochemistry* **1992**, *31*, 65.
(22) Kremer, E. J.; Pritchard, M.; Linch, M.; Yu, S.; Holman, K.; Baker, E.; Warren, S. T.; Schlessinger, D.; Sutherland, G. R.; Richards, R. I. *Science* **1991**, *252*, 1711.
(23) Tchurikov, N. A.; Ebralidze, A. K.; Georgiev, G. P. *EMBO J.* **1986**, *5*, 2341.
(24) Tchurikov, N. A.; Chernov, B. K.; Golova, Y. B.; Nechipurenko, Y. D. *FEBS Lett.* **1989**, *257*, 415.
(25) Tchurikov, N. A.; Shchyolkina, A. K.; Borisova, O. F.; Chernov, B. K. *FEBS Lett.* **1992**, *297*, 233.
(26) Veitia, R.; Ottolenghi, C. *J. Theor. Biol.* **2000**, *206*, 317.
(27) Kandimalla, E. R.; Agrawal, S.; Venkataraman, G.; Sasisekharan, V. *J. Am. Chem. Soc.* **1995**, *117*, 6416.

Parallel DNA duplexes were first found in the crystal structure of a very short, mismatched DNA sequence intercalated by proflavine.[30] Low resolution data of parallel-stranded duplex were found for longer pieces of RNA of sequence poly-[d(A·U)], where the 2-position of adenines was modified by addition of bulky groups.[31] The first structural model of polymeric parallel-stranded duplex DNA was derived by Pattabiraman,[32] who on the basis of theoretical calculations designed a model for the parallel pairing of poly[d(A·T)] duplexes based on the reverse Watson−Crick motif. This model has been confirmed by low[9−15,33] and high resolution[34,35] experimental techniques on d(A·T) rich sequences.

The parallel-stranded duplex model early described by Pattabiraman[32] and further refined by NMR data[12,33,34] shows a general structure not far from the canonical antiparallel B-type helix. The bases are mostly perpendicular to the helix axis, there are two equivalent grooves, sugar units present puckerings in the *South* region, and the A·T pairings are reverse Watson−Crick (Figure 1). This structure—the parallel reverse Watson−Crick (rWC) duplex—is the most stable conformation for parallel-stranded helices rich in d(A·T) pairs, as demonstrated by Jovin and others using a variety of thermodynamic and spectroscopic techniques.[9−15,33] The rWC double helix is less stable than comparable antiparallel helices, but it can be found in hairpins and linear DNAs designed to hinder the formation of the antiparallel d(A·T) helix. The presence of a few d(G·C) steps in the rWC double helix might be tolerated, but it destabilizes the duplex.[14,33]

An alternative structure for parallel-stranded duplexes based on the Hoogsteen (H) recognition mode is also possible (Figure 1). This would lead to a double helix (not yet described from a structural point of view) which might act as a template for triplex formation.[27−29] Parallel-stranded DNA duplexes based on the H pairing occur in duplexes where purines are modified at position 2, which prevents both Watson−Crick and reverse Watson−Crick pairings,[31] or in duplexes rich in d(G·C) (or d(G·G)) pairs. These latter duplexes can exist at neutral pH, but they are especially stable at low pH[16,27−29,36−38] owing to the need to protonate the Hoogsteen cytosine (Figure 1). The stability of the duplex can be also enhanced by DNA-binding drugs such as benzopyridoindole derivatives.[37] Finally, as shown by Lavelle and Fresco[16] and others,[36] H-based parallel duplexes can be more stable than the canonical B-type antiparallel duplex under certain conditions.

In summary, all available experimental data suggest that the structure of parallel-stranded DNAs is quite flexible and can change from H to rWC motifs depending on sequence, pH, and the presence of drugs. Low pH and high content of d(G·C) pairs favor the H-based structure, while the rWC helix is favored in d(A·T) rich sequences and at neutral or basic pH.

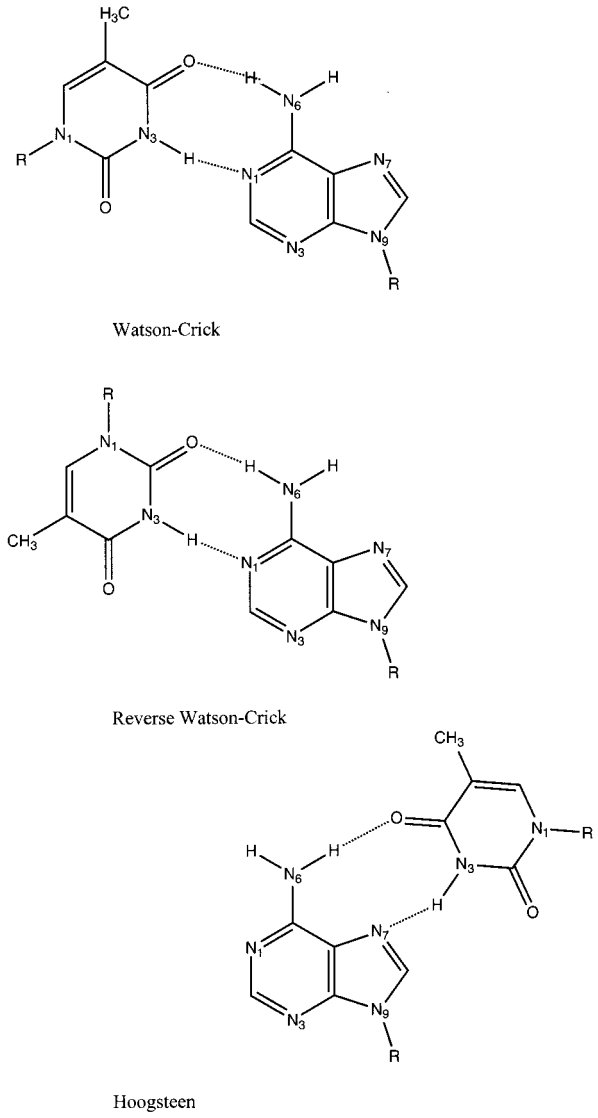

Figure 1. Schematic representation of the Watson−Crick, reverse Watson−Crick, and Hoogsteen A·T pairings.

In this paper we analyze the structure of parallel-stranded duplexes in mixed d(A·T) and d(G·C) sequences using state-of-the-art theoretical calculations and spectroscopic techniques. We also analyze the ability of 8-amino derivatives to stabilize parallel duplexes that can be then used as templates for the formation of triple helices of DNA or DNA−RNA−DNA, which might have a large impact in biotechnological and pharmaceutical research.

Methods

Molecular Dynamics (MD) Simulations. We analyzed the stability of a 11 -mer parallel DNA duplex with almost the same content of d(G·C) and d(A·T) pairs—d(5′-GAAGGAGGAGA-3′)·d(5′-CTTC-CTCCTCT-3′)—in water at room temperature when the base pairing corresponds to both rWC and H motifs. Two and three starting models were considered for H and rWC duplexes, respectively (Table 1). The two starting models for H duplex were obtained by removing the pyrimidine Watson−Crick strand of a A- and B-type triplex (simulations

(28) Kandimalla, E. R.; Agrawal, S. *Biochemistry* **1996**, *35*, 15332.
(29) Aviño, A.; Morales, J. C.; Frieden, M.; de la Torre, B. G.; Güimil-García, R.; Cubero, E.; Luque, F. J.; Orozco, M.; Azorín, F.; Eritja, R. *Bioorg. Med. Chem. Lett.* **2001**, *11*, 1761.
(30) Westhof, E.; Sundaralingam, M. *Proc. Natl. Acad. Sci. U.S.A.* **1980**, *77*, 1852.
(31) Hakoshima, T.; Fukui, T.; Ikehara, M.; Tomita, K. I. *Proc. Natl. Acad. Sci. U.S.A.* **1981**, *78*, 7309.
(32) Pattabiraman, N. *Biopolymers* **1986**, *25*, 1603.
(33) Mohammadi, S.; Klement, R.; Shchyolkina, A. K.; Liquier, J.; Jovin, T. M.; Taillandier, E. *Biochemistry* **1998**, *37*, 16529.
(34) Zhou, N.; Germann, M. W.; van de Sande, J. H.; Pattabiraman, N.; Vogel, H. J. *Biochemistry* **1993**, *32*, 646.
(35) Yang, X. L.; Sugiyama, H.; Ikeda, S.; Saito, I.; Wang. A. H. *Biophys. J.* **1998**, *75*, 1163.
(36) Hashem, G. M.; Wen, J. D.; Do, Q.; Gray, D. M. *Nucleic Acids Res.* **1999**, *27*, 3371.
(37) Escudé, C.; Mohammadi, S.; Sun, J. S.; Nguyen, C.-H.; Bisagni, E.; Liquier, J.; Taillandier, E.; Garestier, T.; Hélène, C. *Chem. Biol.* **1996**, *3*, 57.
(38) Germann, M. W.; Kalisch, G. T.; van de Sande, J. H. *Biochemistry* **1998**, *37*, 12962.

Table 1. Summary of Starting Structures and Simulation Times Used for MD Analysis of Parallel-Stranded Duplexes[a]

pairing scheme	starting structure	length of simuln (ns)
Hoogsteen	modeled from B-type triplex from refs 44−46	5
Hoogsteen	modeled from A-type triplex from refs 44−46	5
rev Watson−Crick	modeled from NMR data from ref 35	2[b]
rev Watson−Crick	modeled from theoretical model in ref 32	1[b]
rev Watson−Crick[c]	from an MD model derived from ref 32	5
Watson−Crick[d]	from canonical model in ref 39	5

[a] In all cases structures were modeled by substitution of the original sequence by the studied one prior to the optimization and equilibration process. In the case of rWC pairs the structures were modeled to show a double hydrogen-bond scheme. [b] Simulation was stopped at that time because the structure of the helix was severely distorted. [c] The original rWC d(A·T) Pattabiraman structure[32] was equilibrated for 1 ns using MD; the sequence was then modified to that of interest, then reoptimized, and reequilibrated. [d] Antiparallel duplex.

H_A and H_B). The three starting models for rWC duplex correspond to (i) the NMR model,[35] (ii) the canonical model reported by Pattabiraman,[32] and (iii) an equilibrated MD rWC d(A·T) duplex (see Table 1). These starting structures lead to simulations rWC_1 rWC_2, and rWC_3, respectively. For comparison purposes an antiparallel B-type duplex of the same sequence was generated using canonical structural parameters.[39] In all cases the duplex was immersed in a box containing 2200−2700 water molecules and sodium ions were added to neutralize the system. Based on previous results[16,27,28,36,40−43] Hoogsteen cytosines were protonated. The hydrated duplexes were then optimized, thermalized, and equilibrated for 130 ps using our standard multistep protocol.[44−46] All the systems were then subjected to 1−5 ns of unrestrained MD simulation at constant pressure (1 atm) and temperature (298 K) using periodic boundary conditions and the particle-mesh Ewald method to account for long-range electrostatic effects.[47,48] SHAKE[49] was used to maintain all the bonds at their equilibrium distances, which allowed us the use of a 2 fs time step for integration. AMBER-98/TIP3P[50−52] and previously developed parameters for protonated cytosines and 8-aminopurines[45,53−56] were used.

Geometrical analysis of the trajectories was performed using exclusively the central 9-mer duplex. For most studies the two trajectories of the H-based duplexes were averaged to obtain a better (10 ns) representation of the duplex. Analysis of possible molecular interactions of DNA was carried out using our cMIP program.[57] Curves[58] and in-house developed software was used for the structural analysis of the trajectories.

Free Energy Calculations. Thermodynamic integration technique coupled to molecular dynamics simulations (MD/TI) was used to analyze the effect of replacing 2′-deoxyadenosine, 2′-deoxyguanosine, and 2′-deoxyinosine by their 8-amino derivatives on the stability of the d(5′-GAAGGAGGAGA-3′)·d(5′-CTTCCTCCTCT-3′) parallel-stranded duplex. For this purpose, mutations were performed between 8-amino-2′-deoxyadenosine and 2′-deoxyadenosine (8AA → A), 8-amino-2′-deoxyguanosine and 2′-deoxyguanosine (8AG → G), and 8-amino-2′-deoxyinosine and 2′-deoxyinosine (8AI → I) in both duplex and single-stranded oligonucleotides. The change in stabilization free energy due to the 8AX → X mutation is determined using standard thermodynamic cycles (Figure 2).

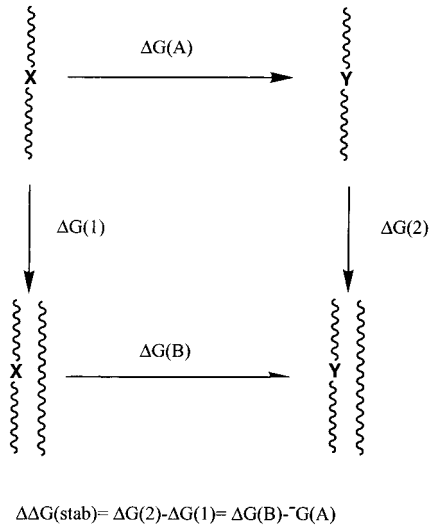

$$\Delta\Delta G(stab) = \Delta G(2) - \Delta G(1) = \Delta G(B) - \Delta G(A)$$

Figure 2. Thermodynamic cycle used to compute the stabilization of parallel-stranded duplexes induced by the introduction of 8-amino derivatives.

MD/TI simulations were done considering only the H duplex due to the instability of the rWC duplex (see below). The starting system in these calculations was defined as that obtained at the third nanosecond of the MD simulation duplex corresponding to the B trajectory of the H duplex. The 8-amino derivatives were then modeled at position 5 (8AG and 8AI) or 6 (8AA) of the purine strand, and the resulting structures were further equilibrated for 0.5 ns to avoid any bias in the calculations. Two additional simulations were performed considering that the d(G·C)/d(I·C) pair at position 5 shows a wobble neutral pairing, $d(G\cdot C)_w/d(I\cdot C)_w$, instead of the normal protonated pair, $d(G\cdot C)^+/d(I\cdot C)^+$. In this case one extra sodium ion was added to the modeled system, which was then further equilibrated for ins. Based on our previous experience,[59,60] the single strands were modeled as 5-mer oligonucleotides of sequences 5′-AG*G*AG-3′, 5′-AG*I*AG-3′, and 5′- GG*A*GG-3′.

Following our standard protocol[53−56,59,60] mutations were performed using 21 double-wide windows of 10 and 20 ps each, leading to trajectories of 420 or 820 ps. Free energy estimates were obtained using

(39) Arnott, S.; Hukins, D. W. L. *Biochem. Biophys. Res. Commun.* **1972**, *47*, 1504.
(40) Lee, J. S.; Johnson, D. A.; Moogan, A. R. *Nucleic Acids Res.* **1979**, *6*, 3073.
(41) Völker, J.; Klump, H. H. *Biochemistry* **1994**, *33*, 13502.
(42) Wittung, P.; Nielsen, P.; Norden, B. *Biochemistry* **1997**, *36*, 7973.
(43) Chollet, A.; Kawashima, E. *Nucleic Acids Res.* **1998**, *16*, 305.
(44) Shields, G.; Laughton, C. A.; Orozco, M. *J. Am. Chem. Soc.* **1997**, *119*, 7463.
(45) Soliva, R.; Laughton, C. A.; Luque, F. J.; Orozco, M. *J. Am. Chem. Soc.* **1998**, *120*, 11226.
(46) Shields, G.; Laughton, C. A.; Orozco, M. *J. Am. Chem. Soc.* **1998**, *120*, 5895.
(47) Essmann, U.; Perera, L.; Berkowitz, M. L.; Darden, T.; Lee, H.; Pedersen, L. G. *J. Chem. Phys.* **1995**, *103*, 8577.
(48) Darden, T. A.; York, D.; Pedersen, L. *J. Chem. Phys.* **1993**, *103*, 8577.
(49) Ryckaert, J. P.; Ciccote, G.; Berendsen, J. C. *J. Comput. Phys.* **1977**, *23*, 327.
(50) Cornell, W. D.; Cieplak, P.; Bayly, C. I.; Gould, I. R.; Merz, K. M.; Ferguson, D. M.; Spellmeyer, D. C.; Fox, T.; Caldwell, J. W.; Kollman, P. A. *J. Am. Chem. Soc.* **1995**, *117*, 5179.
(51) Cheatham, T. E.; Cieplak, P.; Kollman, P. A. *J. Biomol. Struct. Dyn.* **1999**, *16*, 845.
(52) Jorgensen, W. L.; Chandrasekhar, J.; Madura, J. D.; Impey, R.; Klein, M. L. *J. Chem. Phys.* **1983**, *79*, 926.
(53) Soliva, R.; Güimil-García, R. Blas, J. R.; Eritja, R.; Asensio, J. L.; Gonzdlez, C.; Luque, F. J.; Orozco, M. *Nucleic Acids Res.* **2000**, *28*, 4531.
(54) Cubero, E.; Güimil-García, R.; Luque, F. J.; Eritja, R.; Orozco, M. *Nucleic Acid. Res.* **2001**, *29*, 2522.
(55) Güimil-García, R.; Ferrer, E.; Macías, M. J.; Eritja, R.; Orozco, M. *Nucleic Acids Res.* **1999**, *27*, 1991.
(56) Soliva, R.; Luque, F. J.; Orozco, M. *Nucleic Acids Res.* **1999**, *27*, 2248.
(57) Gelpi, J. L.; Luque, F. J.; Orozco, M. *CMIP Computer program*; University of Barcelona: Barcelona, 2001.
(58) Lavery, R.; Sklena, J. *J. Biomol. Struct. Dyn.* **1988**, *6*, 63.
(59) Cubero, E.; Laughton, C. A.; Luque, F. J.; Orozco, M. *J. Am. Chem. Soc.* **2000**, *122*, 6891.
(60) Hernández, B.; Soliva, R.; Luque, F. J.; Orozco, M. *Nucleic Acids Res.* **2000**, *28*, 4873.

the first and second halves of each window, which allows us to have two independent estimates of the free energy change for every simulation. The values presented here correspond then to the average of four independent estimates, which allows us to estimate the statistical uncertainty of the averages. All other technical details of MD/TI simulations are identical to those of MD calculations. We should note that simulations presented here correspond to more than 30 ns of unrestrained MD simulations of 11-mer H duplexes in water. This is to our knowledge one of the most extensive samplings of an anomalous DNA structure published to date.

All MD and MD/TI simulations were carried out using the AMBER-5.1 computer program.[61] All simulations were done in the supercomputers of the Centre de Supercomputació de Catalunya (CESCA) as well as in workstations in our laboratory.

Preparation of Oligomers Containing 8-Aminopurines. Oligonucleotides were prepared on an automatic DNA synthesizer using standard and reversed 2-cyanoethyl phosphoramidites and the corresponding phosphoramidites of the 8-aminopurines. The phosphoramidite of protected 8-amino-2′-deoxyinosine was dissolved in dry dichloromethane to make a 0.1 M solution. The rest of the phosphoramidites were dissolved in dry acetonitrile (0.1 M solution). The phosphoramidite of the hexaethylene glycol linker was obtained from commercial sources. The preparation of 3′−3′ linked hairpins (R-22, R-22A, R-22G, and R-22I) was performed in three parts: First was the preparation of the pyrimidine part, using reversed C and T phosphoramidites and reversed C support (linked to the support through the 5′ end). Next, after the assembly of the pyrimidine part, a hexaethylene glycol linker was added using a commercially available phosphoramidite. Finally, the purine part carrying the modified 8-aminopurines was assembled using standard phosphoramidites for the natural bases and the 8-aminopurine phosphoramidites. For the preparation of 5′∠5′ linked hairpins (B-22, B-22A, B-22G, B-22AG, B-AT, and B-22A control) a similar approach was used. In this case, the purine part was assembled first, followed by the hexaethylene glycol linker. The pyrimidine part was the last part to be assembled using reversed phosphoramidites. Complementary oligonucleotides containing natural bases were also prepared using commercially available chemicals and following standard protocols. After the assembly of the sequences, oligonucleotide supports were treated with 32% aqueous ammonia at 55 °C for 16 h except for oligonucleotides having 8-aminoguanine. In this case a 0.1 M 2-mercaptoethanol solution in 32% aqueous ammonia was used and the treatment was extended to 24 h at 55 °C. Ammonia solutions were concentrated to dryness and the products were purified by reverse-phase HPLC. Oligonucleotides were synthesized on a 0.2 μmol scale and with the last DMT group at the 5′ end (DMT on protocol) to help reverse-phase purification. All purified products presented a major peak, which was collected. Yields (OD units at 260 nm after HPLC purification, 0.2 μmol) were between 6 and 10 OD. HPLC conditions: HPLC solutions are as follows. Solvent A, 5% ACN in 100 mM triethylammonium acetate (pH 6.5); and solvent B, 70% ACN in 100 mM triethylammonium acetate pH 6.5. Columns: PRP-1 (Hamilton), 250 × 10 mm. Flow rate 3 mL/min. A 30 min linear gradient from 10 to 80% B (DMT on), or a 30 min linear gradient from 0 to 50% B (DMT off).

Melting Experiments. Melting experiments were performed as follows: Solutions of the hairpins and duplexes were dissolved in 1 M NaCl, 100 mM phosphate/citric acid buffer. The solutions were heated to 90 °C, they were allowed to cool slowly to room temperature, and then samples were kept in the refrigerator overnight. UV absorption spectra and melting experiments (absorbance vs temperature) were recorded in 1 cm path length cells using a spectrophotometer, which has a temperature controller with a programmed temperature increase of 0.5 °C/min. Melts were run on duplex concentration of 3−4 μM at 260 nm.

Circular Dichroism (CD). Oligonucleotides were disolved in 100 mM phosphate buffer pH 6.0, 50 mM sodium chloride, and 10 mM magnesium chloride. The equimolar concentration of each strand was 4−5 μM. The solutions were heated at 90 °C, allowed to come slowly to room temperature, and stored at 4 °C until CD measurement was performed. The CD spectra were recorded on a Jasco J-720 spectropolarimeter attached to a Neslab RP-100 circulating water bath in 1 cm path length quartz cylindric cells. Spectra were recorded at room temperature using a 10 nm/min scan speed, a spectral bandwidth of 1 nm, and a time constant of 4 s. CD melting curves were recorded at 280 nm using a heating rate of 20 °C/h and a scan speed of 100 nm/min. All the spectra were subtracted with the buffer blank, normalized to facilitate comparisons, and noise- reduced using Microcal Origin 5.0 software.

NMR Spectroscopy. A sample of the oligonucleotide d(3′-AGNG-GNGGAAG-5′-$(EG)_6$-5′-CTTCCTCCTCT-3′) (N = 8-amino-A) for NMR experiments was prepared in 250 μL of 9:1 H_2O/D_2O, 25 mM sodium phosphate buffer, and 100 mM NaCl. The pH was adjusted by adding small amounts of concentrated HCl. The final oligonucleotide concentration was around 1 mM. Spectra were acquired in a Bruker AMX spectrometer operating at 600 MHz, and processed with the UXNMR software. Water suppression was performed by using a jump-and-return pulse sequence with a null excitation in the water signal.[62] All experiments were acquired at 5 °C.

Results and Discussion

Molecular Dynamics Simulations. MD simulations of H duplexes show stable trajectories along the 5 ns simulation time (Figure 3), as noted in the average root-mean-square deviation (rmsd) between the trajectories and the respective MD-averaged conformations (1.4 and 1.5 Å for simulations H_A and H_B, respectively). The only noticeable distortions are a slight bend at the d(G·C) end and the existence of partial fraying events at the d(A·T) end. Note that similar features occur in the control antiparallel helix. It is also worth noting that the existence of two consecutive protonated pairs $d(G\cdot C)^+$ does not introduce large structural alterations in the helix, thus confirming recent MD simulations of triple helices[54] and in agreement with NMR data.[63−70]

The two simulations, which started from different H-based duplex models, are reasonably converged and sample similar regions of the conformational space. This is noted in the rmsd between each trajectory and the MD-averaged conformation of the other: 1.9 Å (B trajectory with respect to the average structure in simulation H_A) and 2.1 Å (A trajectory with respect to the average structure in simulation H_B). Both trajectories sample conformational regions close to those typical of Hoogsteen strands in a triplex DNA (Figure 3). Therefore, MD simulations suggest that the structure of the Hoogsteen strands of a triplex is not largely distorted when the pyrimidine

(61) Case, D. A.; Pearlman, D. A.; Caldwell, J. W.; Cheatham, T. E.; Ross, W. S.; Simmerling, C. L.; Darden, T. A.; Merz, K. M.; Stanton, R. V.; Cheng, A. L.; Vincent, J. J.; Crowley, M.; Ferguson, D. M.; Radmer, R. J.; Seibel, G. L.; Singh, U. C.; Weiner, P. K.; Kollman, P. A. *AMBER 5*; University of California: San Francisco, 1997.

(62) Plateau, P.; Güeron M. *J. Am. Chem. Soc.* **1982**, *104*, 7310.
(63) Rajagopal, P.; Feigon, J. *Biochemistry* **1989**, *28*, 7859.
(64) Rajagopal, P.; Feigon, J. *Nature* **1989**, *339*, 667.
(65) Radhakrishnan, I.; Patel, D. J. *Biochemistry* **1994**, *33*, 1405.
(66) Radhakrishnan, I.; Patel, D. J. *Structure* **1994**, *2*, 395.
(67) Wang, E.; Koshlap, K. M.; Gillespie, P.; Dervan, P. B.; Feigon, J. *J. Mol. Biol.* **1996**, *257*, 1052.
(68) Asensio, J. L.; Dhesai, J.; Bergquist, S.; Brown, T.; Lane, A. N. *J. Mol. Biol.* **1998**, *275*, 811.
(69) Asensio, J. L.; Brown, T.; Lane, A. N. *Structure* **1999**, *7*, 1.
(70) Asensio, J. L.; Brown, A. T.; Lane, A. N. *Nucleic Acids Res.* **1998**, *26*, 3677.

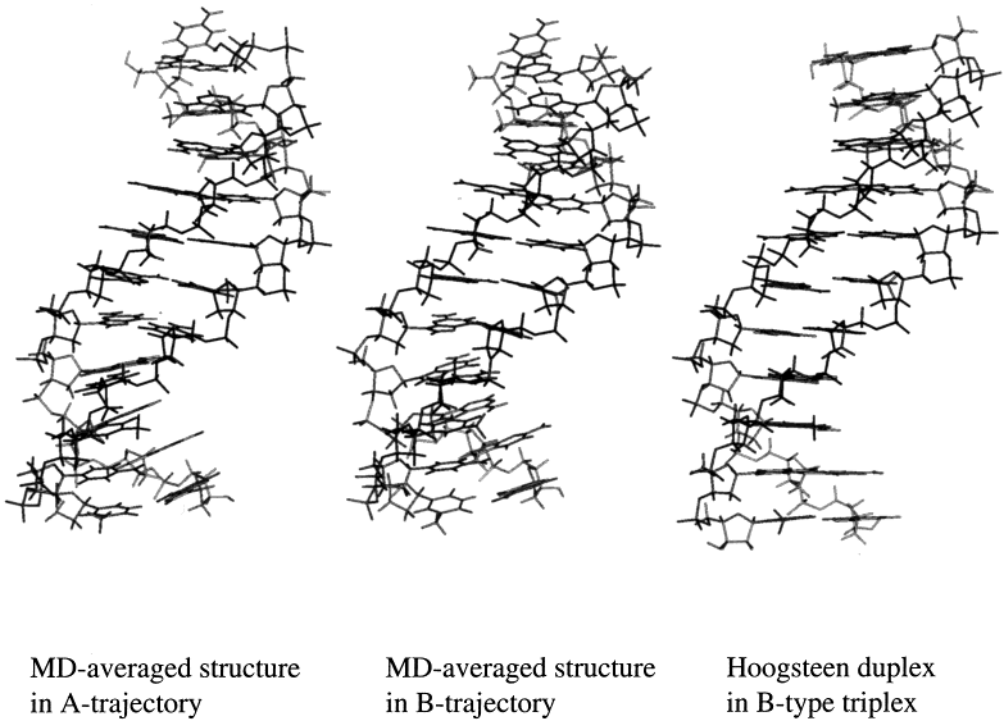

Figure 3. MD-averaged structures of the Hoogsteen duplexes obtained in the A and B trajectories. The conformation of the Hoogsteen duplex in a B-type triplex is displayed for comparison.

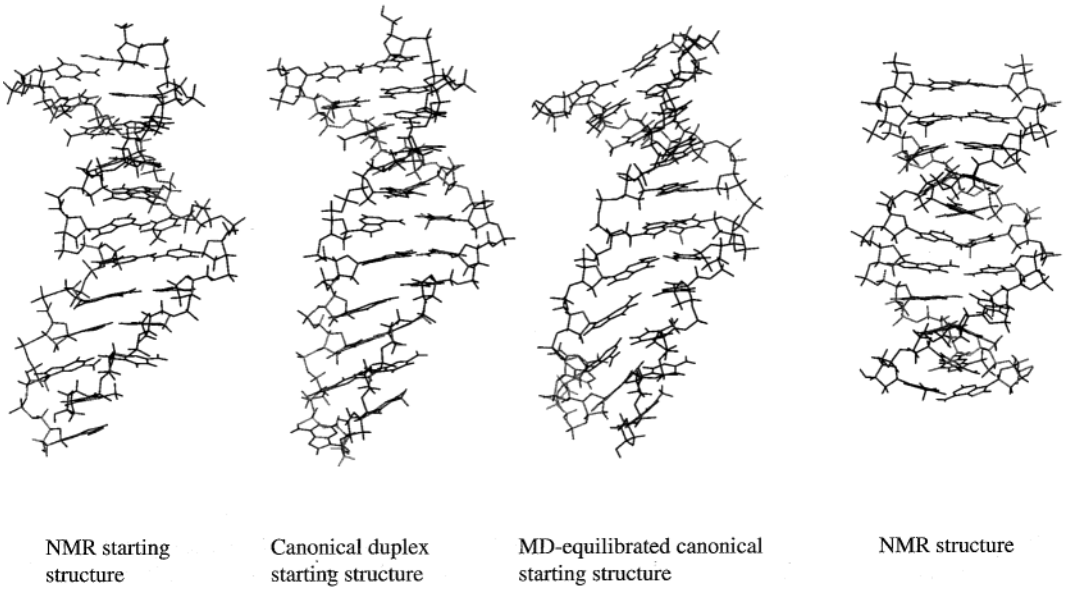

Figure 4. Final structures obtained in the three trajectories of the reverse Watson−Crick duplex (see text). The structure generated from the experimental NMR structure[35] is displayed for comparison.

Watson−Crick strand is removed. Thus, the rmsd between the two trajectories and the starting model in simulation H_B (taken directly from a B-type triplex DNA, ref 45) is 1.4 and 1.8 Å in simulations H_B and H_A, respectively. The rmsd is slightly larger with respect to the Hoogsteen strands of the starting model in simulation H_A (an A-type triplex): 2.0 Å (H_A) and 2.1 Å (H_B).

In contrast to these results, the simulations of rWC duplexes starting from the high-resolution NMR[35] or the canonical[32] model (simulations rWC_1 and rWC_2) diverge very quickly as noted in rmsd profiles (data not shown, but available upon request). All the efforts to reinforce the equilibration of the system and the pairing between bases fail to provide stable structures (rmsd from canonical structure 3.4−3.9 Å at the end of the simulations). Beside the fact that many interstrand hydrogen bonds and stacking interactions are preserved along the simulation, the geometries are heavily distorted in less than 1 ns (see Figure 4), and the helical nature of the structures is then completely lost. The third simulation (rWC_3), which started from a model derived from a previously 1 ns equilibrated trajectory of a d(A·T) rWC duplex, was stable for a longer period, but the helix was also largely distorted (rmsd 3.2 Å) after the 5 ns simulation time (Figure 4). Analysis of the trajectories suggest that the amino repulsion between G and C is the main factor that causes the helix destabilization, despite our efforts to reduce the amino repulsion by promoting a wobble d(G·C) pairing.[33]

The MD simulations strongly suggest that, at least for the sequence considered here, which has almost the same number of d(A·T) and d(G·C) pairs, the rWC duplex is not stable. On the contrary, the H-based conformation seems stable during all the simulation time. Therefore, the results support the existence of H-based motifs for parallel-stranded duplexes in DNAs with similar population of d(A·T) and d(G·C) pairs, and that the rWC helix is not stable when there is a high content of d(G·C) pairs.

The stability of the H-based simulations allows us to analyze the structure of a H-based parallel-stranded duplex. As noted above, the helix is similar to the structure of Hoogsteen strands in a DNA triplex. The average twist is 31°, and the rise is 3.4 Å. The bases are quite perpendicular to the helix axis. The sugars are in the *South* and *South-East* regions, having an average phase angle of 124°, as found experimentally for rWC parallel-stranded duplexes[12,34,35] and triplexes.[44,45,53−56,62−69] There is a narrow groove (denoted "minor" in the following) corresponding to the minor part of the major groove in DNA triplexes,[44] and a wide groove (denoted here "major") corresponding to both the minor groove and the major part of the major groove of a DNA triplex[44] (Figure 3). The shortest P−P average distance along the two grooves is around 9 (±0.6) and 25 (±2) Å for the "minor" and "major" grooves. There are then major differences with rWC duplexes, where two equivalent grooves were found.[32,35]

The classical molecular interaction potential maps (cMIP; Figure 5) allowed us to trace the regions where the DNA has a strong propensity to interact with small cationic probes.[44−46,71] As expected from our previous studies on DNA triplexes,[44,45] the "minor" groove is the most active region for interactions. It is worth noting that the ability of the H duplex to interact with cationic probes is not different from that of a B-type antiparallel duplex with the same sequence, despite the fact that all Hoogsteen cytosines are protonated in the H duplex. It is clear that the short P−P distance in H duplexes creates a strong negative potential in the vicinities of the Hoogsteen cytosines, thus screening their positive charge.

The H duplex is very well hydrated, as shown in the solvation contours represented in Figure 5. The largest apparent density of water is found in the minor groove, which is wide enough to allow the insertion of a chain of ordered waters. There are also regions of large (more than 2 g/mL) water density in the vicinities of the phosphate groups in the major groove. Interestingly, the apparent water densities around the H duplex and the reference antiparallel helix are very similar, thus confirming the findings obtained from cMIP calculations.

In summary, the antiparallel H duplex is a new structure which shares many characteristics with DNA triplexes, but that also exhibits a series of unique molecular recognition characteristics derived mainly from the existence of two very different grooves.

Free Energy Calculations. In a series of previous papers[53−56,72] we reported the design, synthesis, and evaluation of a series of 8-amino derivatives of purine bases. These molecules strongly stabilize the DNA triplex,[53−56,72] which was related, among other factors, to an extra hydrogen bond between the 8-amino group of the purine and the carbonyl group of Hoogsteen cytosines or thymines.[53,54,55] We also found[42] that the 8-amino group promotes a strong destabilization of the Watson−Crick pairing, at least for d(G·C) and d(I·C) pairs. Accordingly, we could expect that the presence of 8-amino groups should destabilize the rWC duplex, increasing the stability of the H duplex. It is worth noting that the stability of the H duplex is crucial for the use of parallel-stranded duplexes as templates for triplex formation. MD/TI calculations were performed only in the H duplex because the instability of the rWC duplex precludes any TI calculation. As found in previous simulations for related systems,[53−56,59,60] the mutation profiles are smooth, without any apparent discontinuity, which could signal the existence of hysteresis. The standard errors in free energy estimates are 0.2−0.3 kcal/mol, thus indicating a good convergence in the results (Table 2).

The H duplex is stabilized by around 2.7 kcal/mol by the A → 8AA mutation (Table 2), a value similar to that found previously[55] using less rigorous simulation protocols for poly d(A−T−T) triplex. The mutation G → 8AG in a d(G−C)$^+$ motif increases the stability of the H duplex by around 1 kcal/mol

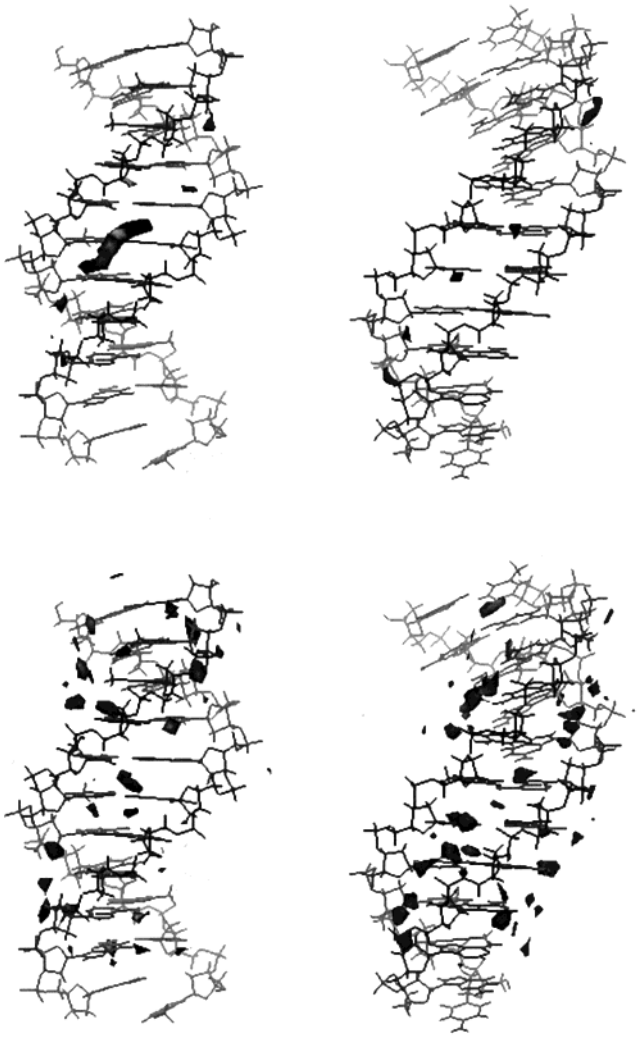

Figure 5. Classical molecular interaction potentials (cMIP; top) and solvation maps (bottom) for the canonical antiparallel duplex (left) and Hoogsteen parallel-stranded duplex (right). cMIP contours correspond to interaction energy of −5 to 5 kcal/mol (O^+ was used as probe). Solvation contours correspond to a density of 2 g/mL. For parallel duplexes cMIP and solvation maps were determined averaging over the A and B trajectories simultaneously.

(71) Gelpi, J. L.; Kalko, S.; de la Cruz, X.; Cirera, J.; Luque, F. J.; Orozco, M. *Proteins* **2001**, *45*, 428.
(72) Güimil-García, R.; Bachi, A.; Eritja, R.; Luque, F. J.; Orozco, M. *Bioorg. Med. Chem. Lett.* **1998**, *8*, 3011.

Table 2. MD/TI Estimates of Stabilization ($\Delta\Delta G_{stab}$ and Standard Errors in kcal/mol) of Parallel-Stranded Duplexes Induced by 8-Amino Derivatives[a]

mutation	complementary pyrimidine	$\Delta\Delta G_{stab}$ (kcal/mol)
G → 8AG	C^+	-1.4 ± 0.2
G → 8AG	C	-3.1 ± 0.3
I → 8AI	C^+	-0.9 ± 0.3
I → 8AI	C	-3.2 ± 0.3
A → 8AA	T	-2.7 ± 0.3

[a] For d(G·C) and d(I·C) motifs the simulation was performed considering two ionization states of the Hoogsteen cytosine. Calculations were carried out always using the sequence d(GAAGXAGGAG), where X is the base which is mutated.

(Table 2), while the I → 8AI mutation in the $d(I-C)^+$ motif increases the stability by around 1.4 kcal/mol (Table 2). These two latter values also agree with previous estimates in DNA triplexes.[53,54] Keeping in mind the similarity between the triplex and the H duplex, this agreement gives confidence to our simulations.

Results noted above clearly point out a strong stabilization of the H duplex upon introduction of 8-aminopurines and suggest that these molecules can help stabilize hairpins based on the parallel H duplex. We were, however, concerned by the fact that the G → 8AG mutation stabilizes the H duplex less than the A → 8AA mutation, since this finding, which agrees with previous calculations in triplexes,[53,54] does not agree with melting experiments on H hairpins (see below). This suggests that when 8AG (or 8AI) is present, the Hoogsteen recognition might not necessarily be the $d(8AG{\cdot}C)^+$ motif, but can be a wobble pair $d(8AG{\cdot}C)_w$ (see Figure 6 and discussion in ref 56). Because the $d(G/I{\cdot}C)^+ \rightarrow d(8AG/8AI{\cdot}C)_w$ mutation is technically very difficult owing to the annihilation of a net charge, we investigated by means of indirect evidence the potential role of $d(8AG{\cdot}C)_w$ and $d(8AI{\cdot}C)_w$ motifs by doing the mutations G → 8AG and I → 8AI in the presence of a neutral cytosine in the complementary Hoogsteen position (the rest of the Hoogsteen cytosines were protonated). The results (see Table 2) suggest that the presence of 8-amino derivatives strongly stabilizes (3.1 and 3.2 kcal/mol for I and G, respectively) the wobble pairing. Note that this free energy difference is 0.5 kcal/mol larger than that found in the A → 8AA mutation and more than 2 kcal/mol larger than the stabilization due to the same mutation when the Hoogsteen cytosine is protonated. According to these results, it can be hypothesized that the presence of 8AG and 8AI favors the existence of neutral Hoogsteen motifs instead of the protonated ones (see below). This could be due to the fact that the 8-amino is a hydrogen-bond donor which interacts better with a neutral molecule than with a cation.

Structure of the Oligonucleotide Derivatives. To check MD and MD/TI- derived hypothesis, several parallel-stranded DNA hairpins carrying 8- aminoadenine (8AA = A^N), 8-aminoguanine (8AG = G^N), and 8-aminohypoxanthine *N* (8AI = I^N) were prepared. The sequences of the oligonucleotides are shown in Figure 7 .[73]

The first group of oligomers are parallel-stranded hairpins connected through their 3′ ends with an hexaethylene glycol linker [$(EG)_6$]. Two adenines are substituted by two 8-amino-

(73) When the nucleotides 8-amino-2′-deoxyadenosine, 8-amino-2′-deoxyguanosine, and 8-amino-2′-deoxyinosine appear in an oligonucleotide, the standard abbreviations (8AA, 8AG, and 8AI) are changed to A^N, G^N, and I^N.

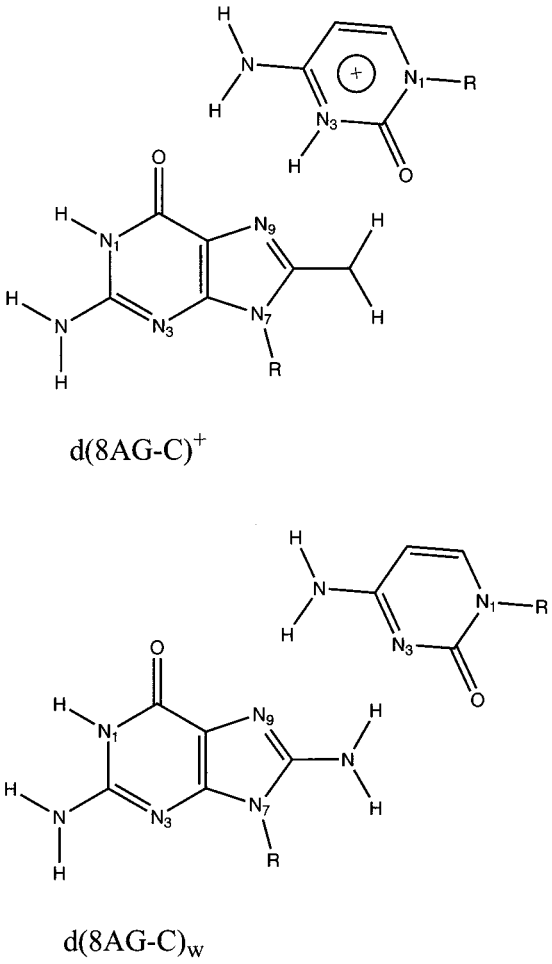

Figure 6. Representation of protonated and wobble Hoogsteen 8AG−C dimers.

R-22	$^{5'}$GAAGGAGGAGA$^{3'}$-$(EG)_6$-$^{3'}$TCTCCTCCTTC$^{5'}$
R-22A	$^{5'}$GAAGG**A^N**GG**A^N**GA$^{3'}$-$(EG)_6$-$^{3'}$TCTCCTCCTTC$^{5'}$
R-22G	$^{5'}$GAAG**G^N**AG**G^N**AGA$^{3'}$-$(EG)_6$-$^{3'}$TCTCCTCCTTC$^{5'}$
R-22I	$^{5'}$GAAG**I^N**AG**I^N**AGA$^{3'}$-$(EG)_6$-$^{3'}$TCTCCTCCTTC$^{5'}$
B-22	$^{3'}$AGAGGAGGAAG$^{5'}$-$(EG)_6$-$^{5'}$CTTCCTCCTCT$^{3'}$
B-22A	$^{3'}$AGA**^{N}**GG**A^N**GGAAG$^{5'}$-$(EG)_6$-$^{5'}$CTTCCTCCTCT$^{3'}$
B-22G	$^{3'}$AGA**G^N**GA**G^N**GAAG$^{5'}$-$(EG)_6$-$^{5'}$CTTCCTCCTCT$^{3'}$
B-22AG	$^{3'}$AGA**^{N}G^{N}GA^{N}G^N**GAAG$^{5'}$-$(EG)_6$-$^{5'}$CTTCCTCCTCT$^{3'}$
B-AT	$^{3'}$AAAAAAAAAAA$^{5'}$-$(EG)_6$-$^{5'}$TTTTTTTTTTT$^{3'}$
B-22Acontrol	$^{3'}$AGA**^{N}**GG**A^N**GGAAG$^{5'}$-$(EG)_6$-$^{5'}$CCCCCTTTTTT$^{3'}$
D1	$^{5'}$ GAAGGAGGAGA$^{3'}$ · $^{5'}$TCTCCTCCTTC$^{3'}$
D2	$^{5'}$ GAAGGAGGAGA$^{3'}$ · $^{5'}$TCCTCCT$^{3'}$

Figure 7. Sequences of parallel-stranded hairpins carrying 8-aminopurines prepared in the present work. A^N, 8-aminoadenine; G^N, 8-aminoguanine; I^N, 8-aminohypoxanthine; $(EG)_6$, hexaethylene glycol linker. Two antiparallel duplexes used as control are also displayed.

adenines (A^N) in the oligonucleotide R-22[a], in the oligonucleotide R-22G two guanines are substituted by two 8-aminoguanines (G^N), and in the oligonucleotide R-22I two guanines are substituted by two 8-aminohypoxanthines (I^N). The oligonucleotide (R-22) contains only the natural bases without modification.

The second group of oligomers (B-22, B-22A, B-22G) is similar in composition to those in the previous oligomers, but the polypurine and the polypyrimidine parts are connected

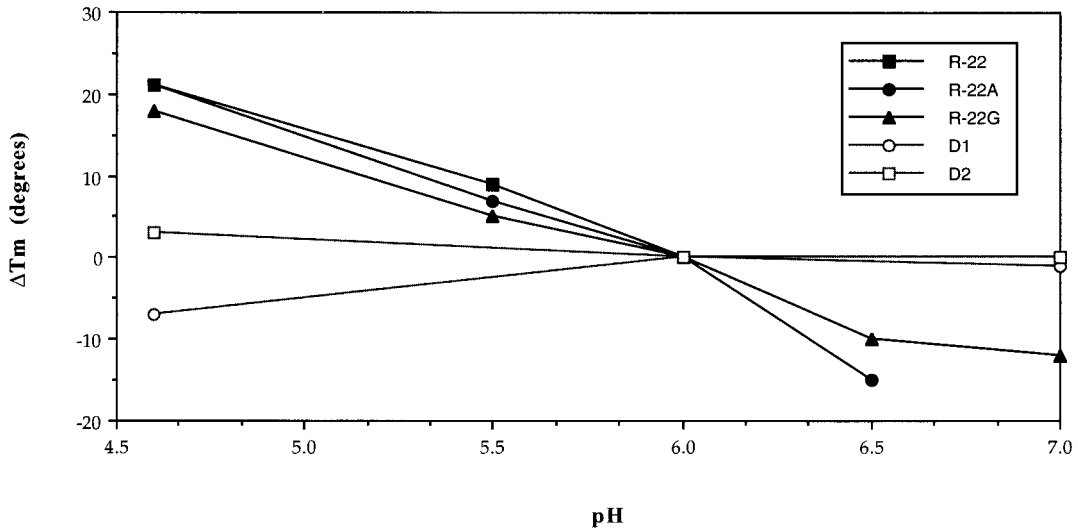

Figure 8. Dependence of T_m with pH for R-22, B-22, and two antiparallel duplexes D 1 and D2 (see Figure 7 for nomenclature).

Table 3. Melting Temperatures[a] (°C) for the Parallel-Stranded Hairpins Having 3′−3′ Linkages

hairpin	pH 4.6	pH 5.5	pH 6.0	pH 6.5	pH 7.0
R-22	46	34	25		
R-22A	64	50	43	28	
R-22G	68	55	50	40	39
R-22I	52	42	34	25	23

[a] In1 M NaCl, 100 mM sodium phosphate/citric acid buffer.

through their 5′ ends with an hexaethylene glycol linker [$(EG)_6$]. In addition, an oligomer having two 8-aminoguanines and two 8-aminoadenines was prepared (B-22AG) to test whether the stabilizing properties of both 8-aminopurines are additive. A parallel-stranded hairpin that has only d(A·T) base pairs (B-AT) was prepared. Finally, a control hairpin (B-22A control) with the same purine sequence as B22A but a noncomplementary pyrimidine sequence was also prepared.

Oligonucleotide sequences containing 8-aminopurines were prepared using phosphoramidite chemistry on an automatic DNA synthesizer. The parallel-stranded oligomers were prepared following previously described protocols.[9,10,28] The phosphoramidites of 8-aminoadenine, 8-aminoguanine, and 8-aminohyoxanthine were prepared as described previously.[54,55,72,74−76]

Melting Experiments. The relative stability of parallel-stranded hairpins was measured spectrophotometrically at different pHs (pH 4.6−7.0). In most cases one single transition was observed with an hyperchromicity around 15% at acidic pH and 10% at neutral pH that was assigned to the denaturation of the parallel-stranded hairpin. In Table 3 melting temperatures of the hairpins having 3′∠3′ linkages are shown.

When the hairpin is formed by natural bases (R-22), a clear transition is observed at pH 4.6 and pH 6.0 but no transition was observed at pH higher than 6.0. Melting temperatures are pH-dependent, and at lower pH melting temperatures are higher than at pH 7.0. These results are consistent with a Hoogsteen base pairing in where C has to be protonated (i.e., an H-type duplex is supported). This profile of pH dependence cannot be explained for a reverse Watson−Crick parallel duplex, and it is also inconsistent with the existence of short antiparallel duplexes (like a 7-mer duplex d(-AGGAGGA-)·d(-TCCTCCT-), which could be formed with the central part of sequence. To verify the latter point we synthesized and measured the melting temperatures at pH 4.5, 6.0, and 7.0 of two antiparallel duplexes of sequences d(GAAGGAGGAGA)·d(TCTCCTCCTTC) (D1) and d(GAAGGAGGAGA)·d(TCCTCCT) (D2). The profiles of pH dependence with the temperature found for both antiparallel duplexes are compared in Figure 8 with those found for R-22 and B-22. It is clear that the profiles strongly support that the antiparallel duplex is not significantly populated in our experiments.

The substitution of two A's by two 8AAs stabilizes the parallel-stranded structure as seen by the higher melting temperatures at pH 4.6 and 6.0 (ΔT_m 16−18 °C) and the observation of a transition at pH 6.5. The substitution of two G's by two 8AGs raises the melting temperatures of the hairpins even higher. The differences in melting temperatures with respect to B-22 are between 21 and 25 °C. It is also possible to observe a transition at pH 7.0 and 6.5. The substitution of two G's by two 8AIs stabilizes the parallel-stranded structure, but this stabilization is of small intensity (ΔT_m 6−9 °C at pH 4.6−6.0). Finally, it is worth to note that the melting temperatures of hairpins having 8AG and 8AI are not decreasing so quickly at neutral pH. This indicates that these hairpins are not as dependent as the other hairpins to protonation of C probably due to the extra hydrogen bond between the 8-amino group of the 8-aminopurines and the 2-keto group of C.[53−55]

As noted above, in addition to the hairpins linked by 3′∠3′ bonds (R-22 derivatives), we prepared hairpins linked by 5′∠5′ bonds (B-22 derivatives). Table 4 shows the melting temperatures of these hairpins at different pHs.

Results are similar to that described above with hairpins having 3′−3′ linkages. Substitution of A or G by the corresponding 8-aminopurine derivative induces a strong stabilization of the hairpin seen as a higher T_m at acidic pH and the observation of transitions at neutral pH that are not possible to observe with hairpins having only natural bases. It is important to notice also that the addition of both 8AA and 8AG in the same oligonucleotide (B-22AG) has additive effects. For

(74) Kawai, K.; Saito, I.; Sugiyama, H. *Tetrahedron Lett.* **1998**, *39*, 5221.
(75) Rao, T. S.; Durland, R. H.; Revankar, G. R. *J. Heterocycl. Chem.* **1994**, *31*, 935.
(76) Rieger, R. A.; Iden, C. R.; Gonikberg, E.; Johnson, F. *Nucleosides Nucleotides* **1999**, *18*, 73.

Table 4. Melting Temperatures[a] (°C) for the Parallel-Stranded Hairpins Having 5′−5′ Linkages

hairpin	pH 4.6	pH 5.5	pH 6.0	pH 6.5	pH 70
B-22	57	35	25		
B-22A	61	47	38	23	
B-22G	65	54	44	30	21
B-22AG	72	62	52	43	39

[a] In 1 M NaCl, 100 mM sodium phosphate/citric acid buffer.

example, at pH 6.0, the presence of two 8AAs gives an increase on the T_m of 13 °C, two 8AGs give an increase of 19 °C, and the addition of both two 8AAs and two 8AGs gives an increase of 27 °C. The low dependence of melting temperatures with the pH found for values close to pH 7.0 for hairpins having 8AG (R-22G) and 8AI (R- 22I) is observed for hairpin B-22AG, but not for hairpin B-22G. Parallel hairpins containing only A−T pairs (B-AT) had the same melting temperature (T_m = 42 °C) from pH = 5.5 to 7.0. Control hairpin (B-22A control) had no transition at any pH.

All the melting experiments described in Tables 3 and 4 were performed at 1 M NaCl, as described under Methods. In addition, we have performed melting experiments from 0 to 1 M NaCl. Melting temperatures remain unchanged within 1 degree error, in agreement with previous results regarding salt effects in Hoogsteen pairing.[19,77]

It is worth noting the excellent agreement between MD/TI calculations derived from the assumption of an H-type parallel duplex and experimental measures. The large stabilization found theoretically for the amino groups is also detected experimentally in increases in T_m of almost 10 °C per substitution. Interestingly, the greater stability obtained for the G → 8AG mutation compared with that obtained by the A → 8AA mutation and the smaller dependence on pH of the stability of duplexes containing 8AG suggest that neutral wobble pairing might play a key role in parallel duplexes containing d(8AG·C) pairs. Finally, the small stabilization obtained for the G → 8AI mutation is the result of the balance between the stabilization of the H-duplex induced by the I → 8AI mutation and the destabilization induced by the G → I change.[54]

As noted in a previous work,[54] the 8-amino group destabilizes the Watson−Crick pairing for G and I and is expected then to destabilize the reverse Watson−Crick pairing. Accordingly, the stabilization in the duplex structure found experimentally can be understood only considering that the hairpins studied here have a Hoogsteen and not a reverse Watson−Crick secondary structure. Note also that the change in stability of the duplex induced by the G → 8AG or A → 8AA substitutions also argue strongly against the existence of significant amounts of a 7-mer antiparallel duplex. Thus, the changes of two G's (positions 5 and 8) by two 8AGs lead to a decrease of 7 °C in T_m for the two antiparallel duplexes used as controls d(GAAGGAGGAGA)·d(TCTCCTCCTTC) and d(GAAGGAGGAGA)·d(TCCTCCT), while for R-22 and B-22 the same changes induced increase more than 21 °C in T_m.

Circular Dichroism. To obtain information on the structure of the hairpins, circular dichroism spectra were measured. Figure 9A shows the CD spectra of hairpins B-22, B-22A, and B-22G and the parallel-stranded hairpin with d(A·T) base pairs (B-AT). As an additional control, we introduced a modified B22 hairpin (B-22A control), where the sequence of the pyrimidine strand is random, to guarantee that no parallel duplex can be formed. This later oligonucleotide was paired with the corresponding 11-mer oligonucleotide complementary to the WC purine strand (S11WC). As noted in Figure 9B, B-22A control does not have structure, but it generates an antiparallel duplex if a suitable single-stranded oligonucleotidic strand (S11WC) is added (B-22A control + S11WC).

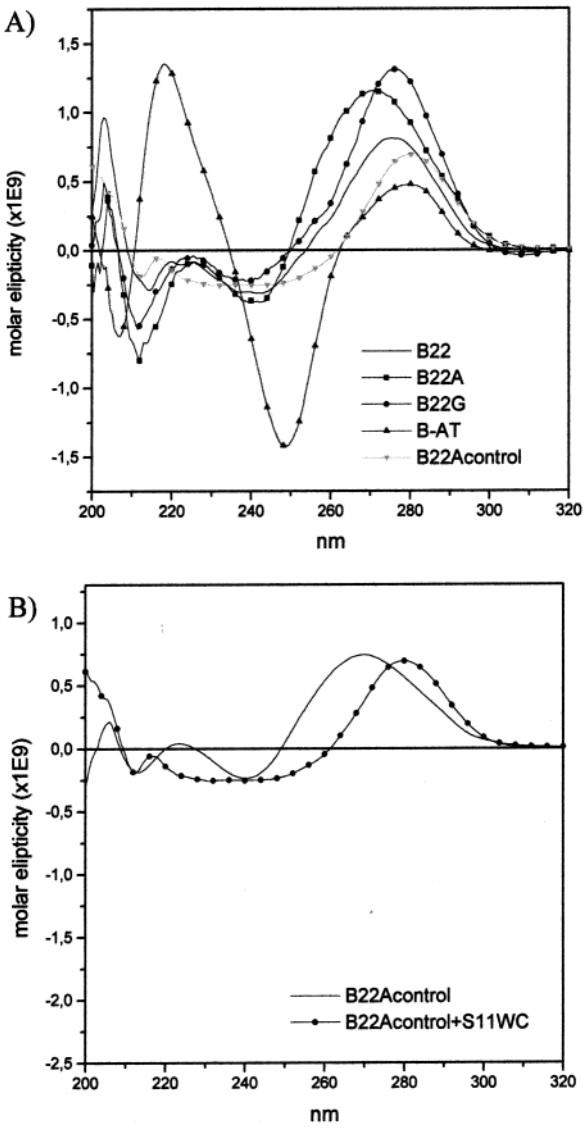

Figure 9. (A) CD spectra of hairpins B-22, B-22A, B-22G, B-AT, and an antiparallel duplex formed by B-22A control (B-22 hairpin where the sequence of the pyrimidine strand is random) and a suitable single-stranded oligonucleotide (S11WC). (B) CD spectra of B-22A control alone and after addition of the antiparallel complementary pyrimidine strand (0.1 M sodium phosphate pH 6.0, 50 mM NaCl, 10 mM $MgCl_2$).

The shapes of the CD spectra (see Figure 9A) of hairpins B-22, B-22A, and B-22G are similar, and clearly differ from B-AT and from the antiparallel duplex (B-22Acontrol + S11WC; see also Figure 9B). The CD spectra of the hairpin B-AT has a strong minimum at 248 nm, a smaller minimum at 206 nm, and two maxima at 218 and 280 nm. This spectrum is similar to that described previously for A−T rich parallel-stranded DNA[9,10,28,78] that is considered a model for reverse Watson−Crick pairing. The CD spectra of B-22, B-22A and

(77) Sugimoto, N.; Wu, P.; Hara, H.; Kawamoto, Y. *Biochemistry* **2001**, *40*, 9396.

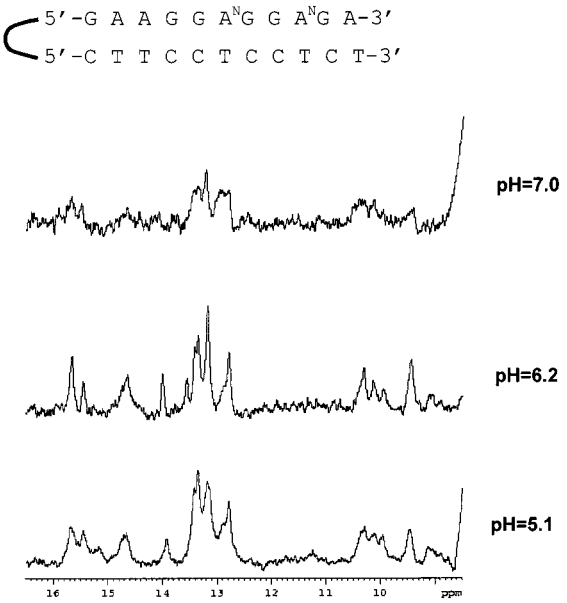

Figure 10. Exchangeable proton region of the NMR spectra of: d(3′-AGA^{N}GGA^{N}GGAAG-5′-$(EG)_6$-5′-CTTCCTCCTCT-3′) at $T = 50$ °C.

B-22G have a strong maximum between 270 and 290 nm and two minima: one at 242 nm and a second, more intense minima at around 212 nm. The minimum around 212 and the maximum around 280 are more intense in the hairpins containing 8-aminopurines (B-22A and B-22G). This type of spectra is characteristic of DNA triplexes.[19] In summary, CD spectra demonstrate that the hairpins studied here, which contains a mixture of A(8AA)−T and G(8AG/8AI)−C steps have a Hoogsteen-type structure and are not reverse Watson−Crick parallel or Watson−Crick antiparallel duplexes.

NMR Spectra. The imino region of one-dimensional ^{1}H NMR spectra of the DNA hairpin d(3′-AGA^{N}GGA^{N}GGAAG-5′-$(EG)_6$-5′-CTTCCTCCTCT-3′) at three different pH's is shown in Figure 10. Unfortunately, the broad signals observed (due probably to the formation of Hoogsteen parallel intermolecular duplexes at the concentration of NMR experiment) prevented the acquisition of high-quality two-dimensional spectra, and, therefore, the sequential assignments could not be done. However, the presence of imino signals between 14.5 and 16.0 ppm clearly indicates that some cytosines are protonated. Also, the signals around 10 ppm correspond to amino protons of cytosines forming Hoogsteen base pairs. Most probably, the resonances around 13 ppm are due to imino protons of Hoogsteen thymines. Since the chemical shifts of the exchangeable protons in reversed Watson−Crick base pairs are very similar to those observed in canonical antiparallel duplexes,[34,79] this kind of base pairing can be ruled out. Finally, it is worth noting that most of the features of the exchangeable proton spectra can be still observed at neutral pH, suggesting a notable stability of the parallel duplex at neutral pH.

Overall, NMR experiments confirm MD, MD/TI, and CD results, and they demonstrate that the parallel-stranded duplexes studied here are stable and show a Hoogsteen-type hydrogen-bonding pattern similar to that of DNA triplexes. The reverse Watson−Crick model of the parallel-stranded duplex, or the standard antiparallel duplex, is ruled out.

Conclusions

Very extended molecular dynamics simulations fail to provide stable helical structures for sequences containing similar number of d(A·T) and d(G·C) pairs arranged in the reverse Watson−Crick structure. On the contrary, stable trajectories are found if a Hoogsteen pairing is assumed. The structures obtained in these trajectories allowed us to describe the structure of an H-type parallel duplex, whose overall conformation is close to that displayed by the Hoogsteen strands of a DNA triplex. CD spectra support this hypothesis, which also agrees with preliminary NMR experiments.

8-Amino derivatives compounds are able to largely increase the stability of DNA hairpins containing almost the same number of d(A·T) and d(G·C) duplexes, which are designed to have a parallel arrangement. This increase in stability is accurately represented by state-of-the-art MD and MD/TI calculations when a Hoogsteen-type secondary structure is assumed for the hairpins.

Overall, the combination of accurate theoretical calculations and experimental techniques has led us to the development of a new strategy for the stabilization of parallel-stranded H-type duplexes. The introduction of 8-amino derivatives can make stable H duplexes under pH or temperature conditions where the helices will be otherwise unstable. These structures can act as templates for the formation of DNA−DNA−DNA and DNA−RNA−DNA triplexes in physiological conditions, which might be useful for biotechnological purposes, as well as for antigene and antisense therapies.

Acknowledgment. We thank the Dirección General de Investigación Científica y Técnica (Projects PB98-1222, BQU2000-0649, and PM99-0046), Generalitat de Catalunya (SGR/00018) and CyGene Inc., for financial support. We also thank the Centre de Supercomputació de Catalunya (CESCA) for computational facilities.

JA011928+

(78) Shchyolkina, A. K.; Borisova, O. F.; Livshits, M. A.; Pozmogova, G. E.; Chernov, B. K.; Klement, R.; Jovin, T. M. *Biochemistry* **2000**, *39*, 10034−10044.

(79) Germann, M. W.; Zhou, N.; van de Sande, J. H.; Vogel, H. J. *Methods Enzymol.***1995**, *261*, 207.